

A Developability-Focused Optimization Approach Allows Identification of in Vivo Fast-Acting Antimalarials: *N*-[3-[(Benzimidazol-2-yl)amino]propyl]amides

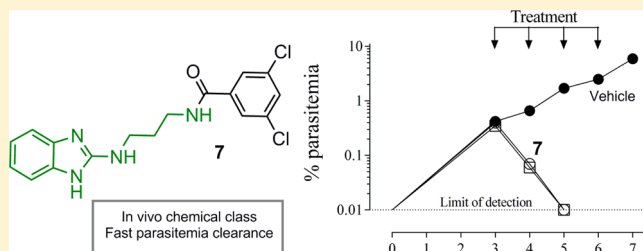
Leena Keurulainen,[†] Mikko Vahermo,[†] Margarita Puente-Felipe,[‡] Elena Sandoval-Izquierdo,[‡] Benigno Crespo-Fernández,[‡] Laura Guijarro-López,[‡] Leticia Huertas-Valentín,[‡] Laura de las Heras-Dueña,[‡] Teppo O. Leino,[†] Antti Siiskonen,[†] Lluís Ballell-Pages,[‡] Laura M. Sanz,[‡] Pablo Castañeda-Casado,[‡] M. Belén Jiménez-Díaz,[‡] María S. Martínez-Martínez,[‡] Sara Viera,[‡] Paula Kiuru,[†] Félix Calderón,^{‡,§} and Jari Yli-Kauhaluoma^{*,†}

[†]Faculty of Pharmacy, Division of Pharmaceutical Chemistry and Technology, University of Helsinki, Viikinkaari 5 E (P.O. Box 56), FI-00014 Helsinki, Finland

[‡]Tres Cantos Medicines Development Campus, GlaxoSmithKline, Severo Ochoa 2, Tres Cantos, Madrid 28760, Spain

Supporting Information

ABSTRACT: Malaria continues to be a major global health problem, being particularly devastating in the African population under the age of five. Artemisinin-based combination therapies (ACTs) are the first-line treatment recommended by the WHO to treat *Plasmodium falciparum* malaria, but clinical resistance against them has already been reported. As a consequence, novel chemotypes are urgently needed. Herein we report a novel, in vivo active, fast-acting antimalarial chemotype based on a benzimidazole core. This discovery is the result of a medicinal chemistry plan focused on improving the developability profile of an antichlamydial chemical class previously reported by our group.



INTRODUCTION

Malaria is an infectious disease caused by parasite of the genus *Plasmodium* associated with nearly 600,000 deaths in 2014.¹ Five species are known to affect humans: *P. falciparum*, *P. ovale*, *P. malariae*, *P. vivax*, and *P. knowlesi*. The infection is triggered by a female *Anopheles* mosquito blood meal, where infective forms of the parasite are injected into the bloodstream of a mammalian host. In the liver, these forms will develop schizonts and subsequently infective merozoites, which will be released into the bloodstream, invading the red blood cells. It is at this stage when the symptoms of the disease start to be evident. These symptoms include chill, fever, or even cause death.² According to the WHO, Africa represents 90% of the deaths reported, 78% of which are associated with children under the age of five. Malaria is also hampering the economic development in countries affected because of expenditures on prevention and treatments.³

The current recommended treatment by the WHO, artemisinin-based combination therapies (ACTs), are increasingly at risk of resistance development. It is now almost six years since the first data for artemisinin resistance were reported in the Southeast Asia.⁴ This situation highlights the urgent need to find new drugs to treat the disease.

Although chronic underinvestment and a very limited number of clinically validated modes of action have

complicated our ability to discover and develop novel antimalarials (the last new chemical entity, atovaquone, was launched more than 30 years ago), the public release of novel antiplasmodial data sets is opening up new opportunities for both drug discovery and target identification programs. These sets are the result of the screening of the corporate collections of GlaxoSmithKline (GSK; Tres Cantos Antimalarial set, TCAMS),⁵ Novartis,⁶ and St. Jude Children's Research Hospital.⁷ The three sets are available for download from the ChEMBL-NTD database.⁸ Subsequent in-depth analysis of the GSK set resulted in the characterization of 5 out of the 47 chemical classes released as benzimidazole scaffolds (Figure 1).^{9–11}

In general, the benzimidazole core can be regarded as a reasonable scaffold from a drug discovery point-of-view, as shown by the high number of hits, leads, and even clinical candidates belonging to this space.¹² Furthermore, various benzimidazole-derived compounds have been recently studied as antiplasmodial agents.^{13–20} Herein we report design and synthesis of the *N*-[3-[(benzimidazol-2-yl)amino]propyl]-amides, evaluation of their antimalarial activity, and further

Received: January 21, 2015

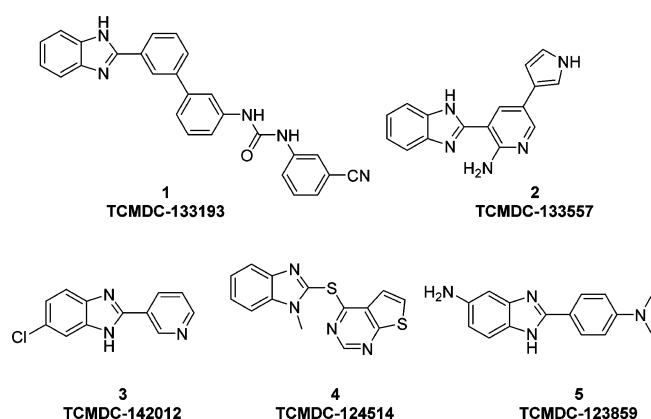


Figure 1. Benzimidazole representatives from the GlaxoSmithKline antimalarial set.

pharmacokinetic and antimalarial in vivo studies for the selected compound.

RESULTS AND DISCUSSION

The benzimidazole derivatives of TCAMS gave inspiration to screen a set of benzimidazole-containing compounds from the University of Helsinki (designed originally as antichlamydia agents)²¹ against *P. falciparum*. Testing delivered the novel antimalarial scaffold **6** (Figure 2). However, **6** presented a weak antiplasmodial potency, a high degree of planarity because of the presence of several aromatic rings, high lipophilicity, scarce solubility, and potential to deliver aniline-like genotoxic metabolites (Table 1).

With the aim of identifying a more developable hit, we focused our attention first on the central unit (Figure 2, Phase I). The hypothesis behind the selection of this first point of synthetic intervention was based on the possibility that having a

flexible linker between the left- and right-hand sides of the molecule could result in compounds with reduced lipophilicity and improved solubility. Simultaneously, we tried to mitigate the genotoxicity risk associated with potential aniline formation by removing the aromatic moiety. A broad variety of aliphatic linkers were prepared (Table 2). The diversity explored includes cyclic groups (**12a–c**) and saturated chains, inspired by the TCAMS antimalarial compounds. Chains with different lengths (**12d–f**) and substitutions (**12g–m**) were explored. The three-carbon linker (**7**) resulted in the most promising substitution, showing 1 order of magnitude improvement in potency (Pf IC_{50} = 0.094 μ M, Tables 1 and 2) and a 3-fold increase in solubility (CLND method, Table 1). Encouragingly, the oral bioavailability, in vivo clearance in mice, and in vitro permeability data associated with this compound were promising (F = 81%, Cl = 39.7 mL/min·kg, and permeability = 380 nm/s; cf. pharmacokinetic data in Supporting Information, Table 1). Interestingly, the solubility in simulated fasting-intestine fluids (FaSSIF solubility) was found to be above 100 μ g/mL.

Compound **7** and its analogs (Table 3) can be easily accessed by heating the mixture of 2-chlorobenzimidazole and the corresponding diamine alkyl derivative without solvent. The target compounds are obtained by a standard amide coupling reaction with EDC and the desired aromatic carboxylic acid (Scheme 1A). SAR exploration of the molecule's left-hand side was undertaken by reacting the isothiocyanate **21** with various *o*-diaminobenzenes in the presence of DCC (Scheme 1B).

Although compound **7** presents an in vitro selectivity index of 386, the impact of further reduction in lipophilicity was explored (Figure 2, Phase II). Efforts to increase polarity through replacement of one halogen atom or, alternatively, through the introduction of different heterocycles resulted in a decreased potency (Table 3). However, combination of the last two strategies afforded **8** (Figure 2). This compound presented

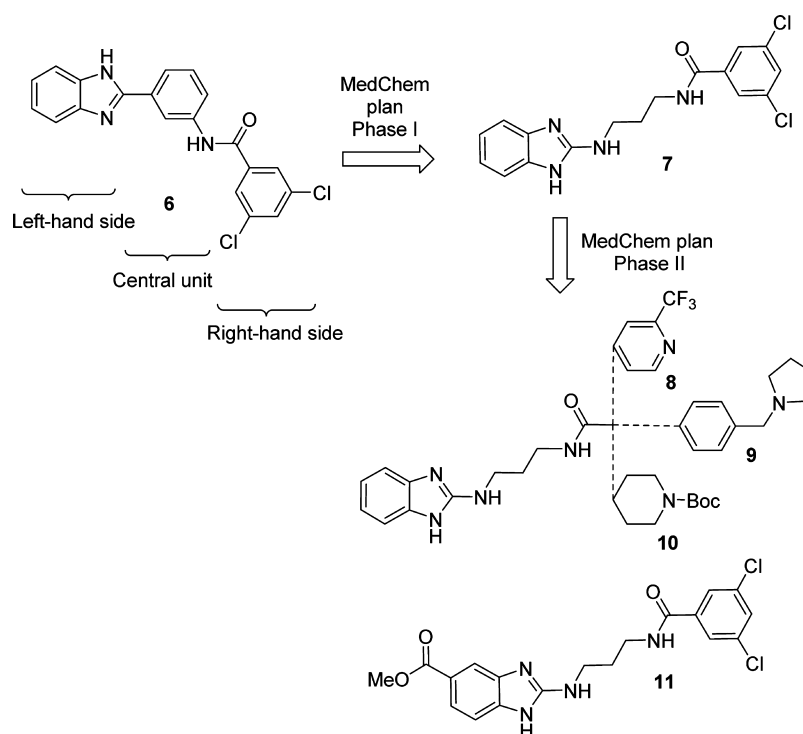


Figure 2. Medicinal chemistry strategy. Figure shows the key analogs.

Table 1. Antimalarial Efficacy against *P. falciparum*, hERG Inhibition, Cytotoxicity, Solubility, and Selectivity Indices of the Key Compounds

compd	<i>Pf</i> IC ₅₀ 3D7A (μM) ^a	<i>Pf</i> IC ₅₀ W2 (μM)	<i>Pf</i> IC ₅₀ V1/S (μM)	hERG inhibition (μM) ^b	HepG2 Tox ₅₀ (μM) ^c	CLND solubility (μM) ^d	SI ^e
6	1.52			>14.79	26.3	64	17.3
7	0.094	0.410	1.029	1.17	36.31	239	386
8	0.25			22.39	>100	349	>400
9	2.30			>50.1	>100	322	>43.5
10	0.90			>50.1	>100	393	>111
11	0.15			>50.1	25.7	29	171
chloroquine	0.036	>1	>1				
pyrimethamine	0.068	>20	>20				

^aAverage of duplicates. *Pf*, *P. falciparum*. ^b50% inhibitory concentration. ^c50% cytotoxic concentration. ^dChemiluminescent nitrogen detection, kinetic solubility from DMSO stock solution in phosphate buffered saline (pH 7.4). ^eSelectivity index (HepG2 tox₅₀/*Pf* IC₅₀).

Table 2. Structures and Antimalarial Activity (*P. falciparum* 3D7A IC₅₀ (*Pf* IC₅₀, μM)) of the Central-Part-Modified Derivatives 7 and 12a–m

X		IC ₅₀	X		IC ₅₀	X		IC ₅₀
12a		2.52	7		0.094	12h		1.38
12b		>5	12e		1.83	12i		1.58
12c		>5	12f		0.40	12j		0.52
12d		>5	12g		4.18	12k		1.03
						12l		1.80
						12m		>5

a competitive potency (*Pf* IC₅₀ = 0.25 μM, Table 1) combined with improved solubility and no signs of cytotoxicity (Tox₅₀ > 100 μM), showing that cytotoxicity is not intrinsically related to the chemical class. Preliminary hERG profiling of compounds 6–11 also suggested differences between the different structures. Classical strategies to improve solubility by the addition of basic amino groups (9, Figure 2) and reduction of aromaticity (10, Figure 2) resulted in compounds with inferior overall profiles when comparing to 8. However, single-digit micromolar antiparasitological activities were measured, warranting further interest in the compound series.

Next, we moved to the left-hand side of the molecule. The benzimidazole positions liable to oxidation were successfully blocked without loss of potency (11, Figure 2 and Table 1), but neither polar substituents nor aza derivatives showed a competitive potency (Table 4). Figure 3 summarizes the key SAR findings during Phase I and II of the optimization process.

At this point, compound 7 was selected for further parasitological profiling in vitro and validation of the series in vivo to classify the type of antimalarial efficacy. The compound was evaluated in a 4 day test using a humanized mouse model.²² Mice were infected at day 0 with the human parasite (*P. falciparum* Pf 3D7^{0087/N9}), and 3 days after infection, the compound was dosed once a day for four consecutive days.

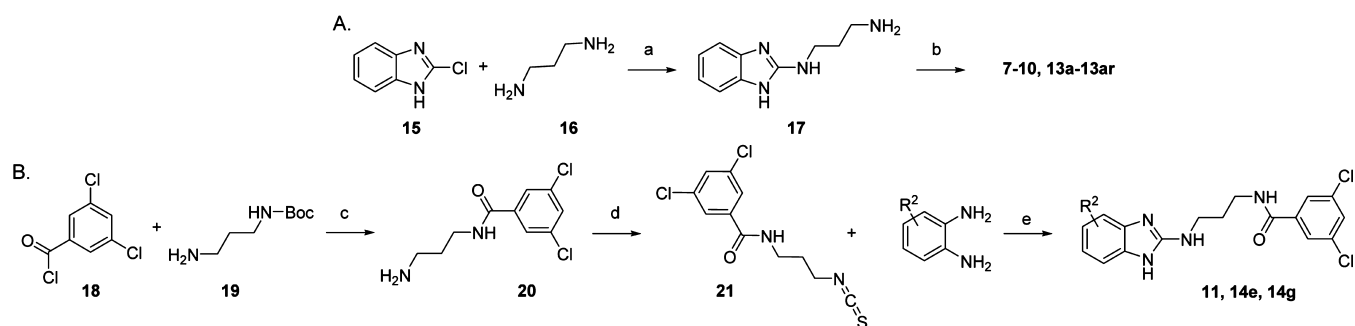
Compound 7 was able to reduce the parasitemia under the limit of detection with just two doses, showing a parasite clearance rate consistent with fast-acting antimalarials like dihydroartemisinin and piperazine (Figure 4A). The microscopic observations suggest that 7 induces rapid in vivo killing of *P. falciparum* erythrocyte stages (pyknotic parasites emerging 2 days after the initiation of treatment, Figure 4B). Regarding its in vitro profiling, the compound was tested against *P. falciparum* laboratory-adapted strains resistant to chloroquine and pyrimethamine (W2 and V1/S), resulting in a decrease in potency (4- and 11-fold, respectively). Given the importance of these findings, further studies will be required to understand the molecular events underpinning this cross-resistance and mechanism of action of these derivatives. Compound 7 was tested also against gametocyte stage of *P. falciparum*,²³ but it did not show activity (>10 μM).

CONCLUSIONS

We have identified a new antimalarial chemotype, *N*-[3-[(benzimidazol-2-yl)amino]propyl]amides, with promising in vivo pharmacokinetics and efficacy, a fast-acting mode of action (comparable to artemisinins), and amenability for optimization from a medicinal chemistry perspective. The remaining challenges for the lead optimization phase will include

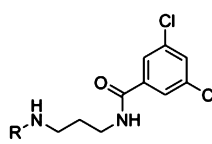
Table 3. Structures and Antimalarial Activity (*P. falciparum* 3D7A IC₅₀ (Pf IC₅₀, μM)) of the Right-Hand Side-Modified Derivatives 8–10 and 13a–ar

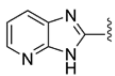
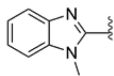
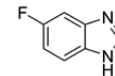
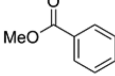
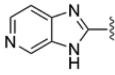
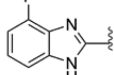
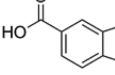
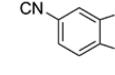
	R	IC ₅₀	R	IC ₅₀	R	IC ₅₀	R	IC ₅₀	
13a		3.17	13m		>5	13y		>5	
13b		0.30	13n		0.32	13z		>5	
13c		1.05	13o		0.33	13aa		1.83	
13d		1.08	13p		0.97	13ab		>5	
13e		4.03	13q		0.93	13ac		2.26	
13f		3.42	13r		0.14	13ad		0.46	
13g		>5	13s		0.37	8		0.25	
13h		1.21	13t		>5	13ae		>5	
13i		0.17	13u		>5	13af		0.10	
13j		0.66	13v		0.38	13ag		1.37	
13k		>5	13w		>5	13ah		>5	
13l		>5	13x		0.63	13ai		2.26	
							13aj		>5
							9		2.30
							13ak		3.26
							13al		3.36
							13am		1.65
							13an		1.80
							13ao		2.64
							13ap		>5
							13aq		>5
							13ar		>5
							10		0.90

Scheme 1. Synthetic Routes for Compounds (A) 7–10 and 13a–ar and (B) 11/14e and 14g^{az}

^aReagents and conditions: (a) 100 °C, 36 h, 66%. (b) R¹COOH, EDC, HOBt, Et₃N, DMF, rt, 1.5–17 h, 3–67%. (c) (1) Et₃N, CH₂Cl₂, 1.5 h, 84%; (2) TFA, CH₂Cl₂, rt, 4 h, 68% over two steps. (d) TCDI, THF, rt, 3 h, quant. (e) DCC, Et₃N, MeCN, 85 °C, 24 h, 18–46%.

Table 4. Structures and Antimalarial Activity (*P. falciparum* 3D7A IC₅₀ (Pf IC₅₀, μM)) of the Left-Hand Side-Modified Derivatives 10 and 14a–g



	R	IC ₅₀	R	IC ₅₀	R	IC ₅₀	R	IC ₅₀			
14a		2.54	14c		>5	14e		0.12	11		0.15
14b		1.06	14d		0.30	14f		>5	14g		1.47

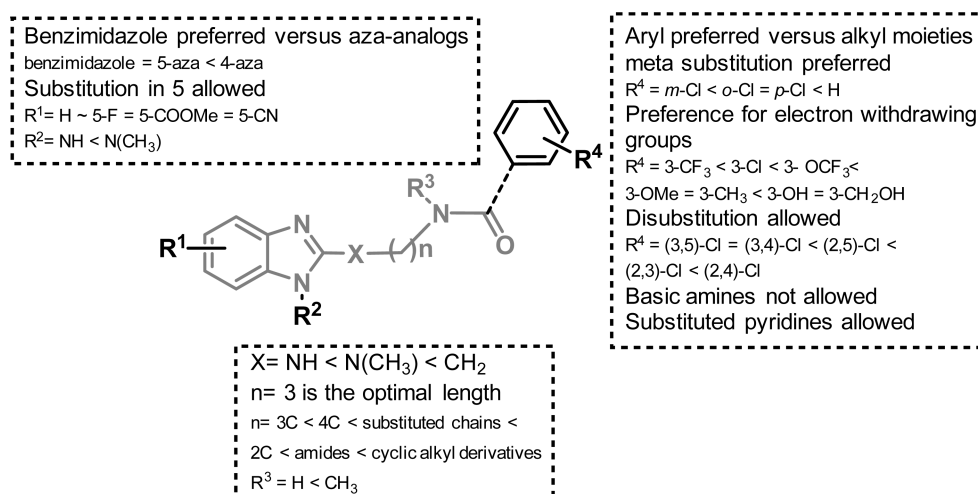


Figure 3. Structure–activity relationships around derivative 7 as antimalarial activity against *P. falciparum* (3D7A), structure, and substituent order are based on Pf IC₅₀. See detailed antimalarial activities of derivatives in Tables 1–4.

mitigation of the observed cardiotoxicity risk (on the basis of values of hERG IonWorks) and understanding of the origin of the cross-resistance observed with W2 and V1/S clones.

EXPERIMENTAL SECTION

Chemistry. LC-MS analyses for purity were performed using a diode-array detector and an ESI ion source. Signal separation was carried out by use of Acquity UPLC BEH C18 column (1.7 μm, 3.0 mm × 50 mm) or Luna C18 (5 μm, 4.6 mm × 50 mm), eluent: 25 mM NH₄OAc + 10% MeCN at pH 6.6/MeCN (gradient run 100:0 → 10:90 for Acquity and 100:0 → 0:100 for Luna), and flow = 0.8 mL/min. Purity of the all tested compounds was 95% or higher.

N-(1*H*-Benz[d]imidazol-2-yl)propane-1,3-diamine (**17**). 1,2-Diaminopropane **16** (8.30 mL, 0.100 mol) and 2-chloro-1*H*-benzimidazole **15** (1.53 g, 10.0 mmol) were heated in sealed tube at 100 °C for 92 h and then evaporated to dryness. Purification by flash-column chromatography (amino column, CH₂Cl₂/MeOH, twice) and recrystallization from MeCN gave compound **17** as off-white crystals (1.30 g, 66%). ¹H NMR (400 MHz, CD₃OD) δ ppm 1.74 (quin, *J* = 7.0 Hz, 2H), 2.69 (t, *J* = 7.1 Hz, 2H), 3.35 (t, *J* = 6.8 Hz, 2H), 6.86–6.90 (m, 2H), 7.08–7.11 (m, 2H).

N-[3-[(1*H*-Benz[d]imidazol-2-yl)amino]propyl]-3,5-dichlorobenzamide (**7**). Compound **17** (0.13 g, 0.70 mmol), EDC (0.15 g, 0.77 mmol), HOBt (0.10 g, 0.77 mmol), Et₃N (0.11 mL, 0.77 mmol), and 3,5-dichlorobenzoic acid (0.14 g, 0.74 mmol) in DMF (6 mL) were stirred at room temperature for 1.5 h. The reaction mixture was partitioned between EtOAc and saturated NaHCO₃, and the organic phase was washed (2×) with H₂O and brine, dried over anhydrous

Na₂SO₄, and evaporated. Purification by preparative HPLC (MeCN/H₂O, NH₄HCO₃) gave compound **7** as off-white powder (0.17 g, 67%). ¹H NMR (400 MHz, CD₃OD) δ ppm 1.94 (quin, *J* = 6.7 Hz, 2H), 3.46 (t, *J* = 6.8 Hz, 2H), 3.50 (t, *J* = 6.8 Hz, 2H), 6.94–6.98 (m, 2H), 7.17–7.19 (m, 2H), 7.63 (t, *J* = 1.8 Hz, 1H), 7.81 (d, *J* = 2.0 Hz, 2H). ¹³C NMR (100 MHz, CD₃OD) δ ppm 30.7, 38.7, 41.3, 121.4, 127.3, 32.3, 136.6, 139.1, 157.1, 167.4. MS: *m/z* 363 [M + H]⁺. Purity was determined as >95% by HPLC (λ 285 nm), R_t: 1.16 min (Acquity UPLC BEH C18 1.7 μm, 3 mm × 50 mm, 25 mM NH₄OAc/MeCN, pH 6.6).

N-[3-[(1*H*-Benz[d]imidazol-2-yl)amino]propyl]-2-(trifluoromethyl)isonicotinamide (**8**). Compound **17** (49 mg, 0.26 mmol), 2-(trifluoromethyl)isonicotinic acid (54 mg, 0.28 mmol), EDC (56 mg, 0.29 mmol), and HOBt (39 mg, 0.29 mmol) were dissolved in dry DMF (3 mL). Et₃N (0.040 mL, 0.29 mmol) was added, and the resulting mixture was stirred at room temperature overnight under N₂. The mixture was poured into H₂O and extracted (3×) with CH₂Cl₂/2-propanol (1:1), washed (2×) with saturated NH₄Cl, dried over anhydrous Na₂SO₄, and evaporated. The crude product was purified with preparative HPLC (H₂O, NH₄HCO₃/MeCN) to give compound **8** as a white solid (17 mg, 17%). ¹H NMR (400 MHz, CD₃OD) δ ppm 1.98 (quin, *J* = 6.69 Hz, 2H), 3.47 (t, *J* = 6.8 Hz, 2H), 3.55 (t, *J* = 6.7 Hz, 2H), 6.96 (m, 2H), 7.17 (m, 2H), 8.01 (d, *J* = 4.8 Hz, 1H), 8.19 (s, 1H), 8.85 (d, *J* = 5.1 Hz, 1H). MS: *m/z* 364 [M + H]⁺. Purity was determined as >95% by HPLC (λ 212 nm), R_t: 1.01 min (Acquity UPLC BEH C18 1.7 μm, 3 mm × 50 mm, 25 mM NH₄OAc/MeCN, pH 6.6).

N-[3-[(1*H*-Benz[d]imidazol-2-yl)amino]propyl]-4-(pyrrolidin-1-ylmethyl)benzamide (**9**). Following the procedure for compound **7**

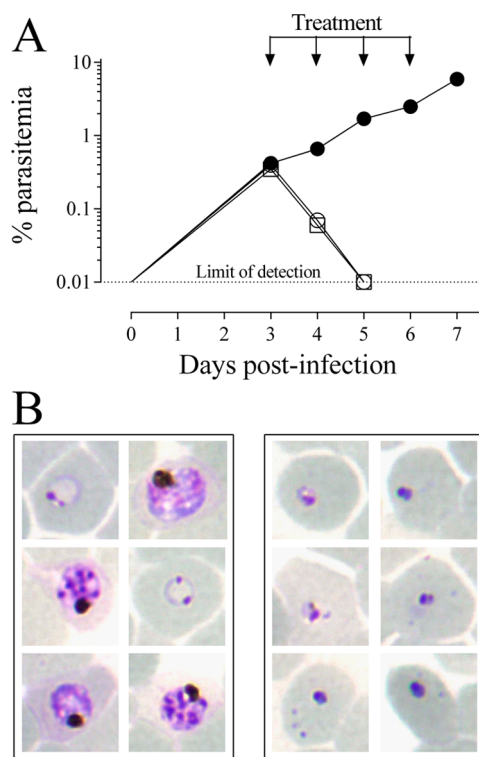


Figure 4. (A) Efficacy of **7** in the *P. falciparum* (*Pf* 3D7^{0087/N9}) mouse model. Data shows individual parasitemia for two mice treated with compound **7** at 100 mg/kg (white dots and squares) or vehicle (black dots). (B) Giemsa-stained peripheral blood smears from mice treated with vehicle (left) and derivative **7** (right) after 48 h starting the treatment.

and using the corresponding carboxylic acid, compound **9** was obtained as a white powder (60 mg, 40%). ¹H NMR (400 MHz, CD₃OD) δ ppm 1.82 (m, 4H), 1.95 (quin, *J* = 6.7 Hz, 2H), 2.56 (m, 4H), 3.47 (t, *J* = 6.8 Hz, 2H), 3.51 (t, *J* = 6.7 Hz, 2H), 3.70 (s, 2H), 6.94–6.97 (m, 2H), 7.17–7.19 (m, 2H), 7.45 (d, *J* = 7.8 Hz, 2H), 7.82 (d, *J* = 8.1 Hz, 2H). MS: *m/z* 378 [M + H]⁺. Purity was determined as >95% by HPLC (λ 212 nm), *R*_f: 0.98 min (Acquity UPLC BEH C18 1.7 μm, 3 mm × 50 mm, 25 mM NH₄OAc/MeCN, pH 6.6).

tert-Butyl 4-[[3-[(1*H*-Benz[d]imidazol-2-yl)amino]propyl]carbamoyl]piperidine-1-carboxylate (**10**). Following the procedure for compound **7**, using the corresponding carboxylic acid and extraction with EtOAc, compound **10** was obtained as a colorless sticky solid (60 mg, 36%). ¹H NMR (400 MHz, CD₃OD) δ ppm 1.46 (s, 9H), 1.57 (qd, *J* = 12.4, 4.0 Hz, 2H), 1.74 (m, 2H), 1.83 (quin, *J* = 6.8 Hz, 2H), 2.36 (m, 1H), 2.78 (br. s, 2H), 3.29 (t, 2H, partially hidden under CD₃OD signal), 3.39 (t, *J* = 6.8 Hz, 2H), 4.10 (m, 2H), 6.96 (m, 2H), 7.18 (m, 2H). MS: *m/z* 402 [M + H]⁺. Purity was determined as >95% by HPLC (λ 212 nm), *R*_f: 1.03 min (Acquity UPLC BEH C18 1.7 μm, 3 mm × 50 mm, 25 mM NH₄OAc/MeCN, pH 6.6).

N-(3-Aminopropyl)-3,5-dichlorobenzamide (**20**). *tert*-Butyl (3-aminopropyl)carbamate **19** (0.34 mL, 2.00 mmol), 2,5-dichlorobenzoyl chloride **18** (0.28 mL, 2.00 mmol), and Et₃N (0.28 mL, 2.00 mmol) in CH₂Cl₂ (10 mL) were stirred at room temperature for 0.5 h. The reaction mixture was partitioned between saturated NaHCO₃ and EtOAc. The organic phase was washed with brine, dried over anhydrous Na₂SO₄, and evaporated. The crude *tert*-butyl [3-(3,5-dichlorobenzamido)propyl]carbamate was obtained as a white solid and was carried to the next step without further purification (0.58 g, 84%). ¹H NMR (400 MHz, CD₃OD) δ ppm 1.36 (s, 9H), 1.68 (quin, *J* = 6.6 Hz, 2H), 3.05 (q, *J* = 6.4 Hz, 2H), 3.33 (t, *J* = 6.8 Hz, 2H), 7.56 (t, *J* = 1.9 Hz, 1H), 7.72 (d, *J* = 1.8 Hz, 2H). A solution of *tert*-butyl [3-(3,5-dichlorobenzamido)propyl]carbamate (1.22 g, 3.51 mmol)

and TFA (2 mL) in CH₂Cl₂ (3 mL) was stirred at room temperature for 4 h, evaporated, and purified by SCX-2 column to give compound **20** as a yellowish solid (0.68 g, 68%). ¹H NMR (400 MHz, CD₃OD) δ ppm 1.76 (quin, *J* = 6.9 Hz, 2H), 2.70 (t, *J* = 6.9 Hz, 2H), 3.44 (t, *J* = 6.8 Hz, 2H), 7.63 (t, *J* = 1.8 Hz, 1H), 7.78 (d, *J* = 2.0 Hz, 2H).

3,5-Dichloro-*N*-(3-isothiocyano)propylbenzamide (**21**). To a suspension of **20** (0.68 g, 2.73 mmol) in dry THF (130 mL) was added 1,1'-thiocarbonyldiimidazole (0.54 g, 3.00 mmol). The resulting mixture was stirred at room temperature for 3 h and washed with brine. The organic phase was dried over anhydrous Na₂SO₄ and evaporated. The resulting oily crude product (1.03 g) was carried to the next step without purification.

Methyl 2-[[3-(3,5-Dichlorobenzamido)propyl]amino]-1*H*-benzimidazole-5-carboxylate (**11**). Compound **21** (0.48 g, 1.65 mmol), methyl 3,4-diaminobenzoate (0.25 g, 1.5 mmol), DCC (0.37 g, 1.8 mmol), and Et₃N (0.21 mL, 1.5 mmol) in MeCN were heated at 85 °C for 24 h and evaporated to dryness. Purification by flash-column chromatography (amino column, MeOH/CH₂Cl₂) gave compound **11** (0.29 g, 46%). ¹H NMR (400 MHz, DMSO-*d*₆) δ ppm 1.82 (quin, *J* = 6.7 Hz, 2H), 3.36–3.40 (m, 4H), 3.80 (s, 3H), 7.01 (br. s, 1H), 7.16 (d, *J* = 8.3 Hz, 1H), 7.58 (d, *J* = 8.1 Hz, 1H), 7.71 (m, 1H), 7.82 (t, *J* = 1.9 Hz, 1H), 7.88 (d, *J* = 1.8 Hz, 2H), 8.8 (m, 1H), 10.90 (m, 1H). ¹³C NMR (100 MHz, DMSO-*d*₆) δ 29.0, 36.8, 39.5, 51.4, 125.8, 130.4, 134.1, 137.6, 163.3, 166.9. MS: *m/z* 421 [M + H]⁺. Purity was determined as >95% by HPLC (λ 208 nm), *R*_f: 1.12 min (Acquity UPLC BEH C18 1.7 μm, 3 mm × 50 mm, 25 mM NH₄OAc/MeCN, pH 6.6).

Biology. *Pf* IC₅₀ Determination. Parasite growth inhibition assays and IC₅₀ determination were carried out following standard methods using the ³H-hypoxanthine incorporation assay.²⁴ Briefly, this assay relies on the parasite incorporation of labeled hypoxanthine that is proportional to *P. falciparum* growth. A culture of *P. falciparum* 3D7 parasitized red blood cells (RBC; 0.5% parasitemia, 2% hematocrit) in RPMI-1640, albumax 5%, and 5 μM hypoxanthine is exposed to serial drug dilutions. Plates are incubated 24 h at 37 °C, 5% CO₂, 5% O₂, 90% N₂. After 24 h of incubation, ³H-hypoxanthine is added, and plates are incubated for additional 24 h period. After that, parasites are harvested on a glass-fiber filter using a TOMTEC Cell harvester 96. Filters are dried and melted on scintillator sheets to determine the incorporation of ³H-hypoxanthine. Radioactivity is measured using a microbeta counter. Data are normalized using the incorporation of the positive control (parasitized RBCs without drug). IC_{50s} are determined using Graft 7 program.

hERG Inhibition Determination and Cell Cytotoxicity Assays. Use of *hERG* channel by IonWorks electrophysiology is described in literature.^{25–27} Cell cytotoxicity assays are described in literature.²⁸

In Vivo Studies. Authors declare that all animal studies were ethically reviewed and approved by the DDW Ethical Committee on Animal Research, performed at the DDW Laboratory Animal Science facilities accredited by AAALAC and carried out in accordance with European Directive 2010/63/EU and the GSK Policy on the Care, Welfare, and Treatment of Animals.

Pharmacokinetic Studies in Mice. For pharmacokinetic studies in mice, animals were dosed by either intravenous (IV) or oral (PO) route. For IV administration, the dosing volume was 10 mL/kg for a total dose of 1 mg/kg, and for PO administration, the dosing volume was 10 mL/kg for a total dose of 10 mg/kg. Dosing solution for intravenous administration was prepared in 20% encapsine and 5% DMSO in saline solution (C = 0.1 mg/mL), and for PO administration, a suspension in 1% methylcellulose (w:v) was formulated (C = 1 mg/mL). Following IV dosing, blood samples were collected at 5, 15, and 30 min and 1, 2, 4, 6, 8, and 24 h postdose. Following oral dosing, blood samples were collected at 15, 30, and 45 min and 1, 2, 4, 6, 8, and 24 h postdose.

For whole blood samples analysis, 25 μL of fresh blood was mixed with 25 μL of saponine solution (0.1% in water) and immediately stored frozen at −80 °C until analysis.

Diluted blood samples were processed under standard liquid–liquid extraction procedures using acetonitrile and analyzed by LC-MS/MS in positive ion mode with electrospray. Samples were assayed for

parent compound using a Sciex API 4000 Triple Quadrupole Mass Spectrometer (Sciex, Division of MDS Inc., Toronto, Canada), against a series of matrix-matched calibration curve standards, using multiple reaction monitoring (MRM) at the specific transitions for the compound. Noncompartmental analysis was performed using Phoenix, version 6.3 (Phoenix WinNonlin, ©1998–2012, Certara L.P.), and the main pharmacokinetic parameters were estimated. Additional statistical analysis of the data was performed with GraphPad Prism, version 5.01 (GraphPad Software Inc., San Diego, CA). Pharmacokinetic parameters are summarized in the Supporting Information.

***P. falciparum* Murine Model.** The efficacy of **7** against *P. falciparum* Pf3D7^{0087/N9} was determined as previously described.²² Briefly, a group of two female NSG (NOD-scid IL-2R^{γnull}) mice engrafted with human erythrocytes (~50% human erythrocytes in peripheral blood) were infected by intravenous route with 2×10^7 parasitized erythrocytes on day 0. The compound was administered per oral route at 100 mg·kg⁻¹ in 1% methylcellulose once a day from day 3 to day 6 after infection. Parasitemia was assessed by FACS as previously described.²⁹ Fresh samples of peripheral blood from *P. falciparum*-infected mice were stained with TER-119-phycoerythrin (marker of murine erythrocytes) and SYTO-16 (nucleic acid dye) and then analyzed by flow cytometry (FACSCalibur, BD). A qualitative analysis of the effect of treatment on *P. falciparum* Pf3D7^{0087/N9} was assessed by microscopy and flow cytometry. Microscopy analysis was performed with Giemsa-stained blood smears as described.¹³ The levels in blood during the 23 h period after the first administration were measured in mice of the efficacy study.

■ ASSOCIATED CONTENT

● Supporting Information

Additional spectroscopic data for **7** and synthetic methodologies for compounds **6**, **12a–m**, **13a–ar**, and **14a–g** as well as additional biological data. The Supporting Information is available free of charge on the ACS Publications website at DOI: 10.1021/acs.jmedchem.5b00114.

■ AUTHOR INFORMATION

Corresponding Author

*E-mail: jari.yli-kauhaluoma@helsinki.fi. Phone: +358-294159170.

Present Address

[§]F.C.: Immuno-inflammation Therapy Area Unit R&D, GlaxoSmithKline, GlaxoSmithKline Medicines Research Center, Gunnels Wood Road, Stevenage, Hertfordshire SG1 2NY, United Kingdom.

Notes

The authors declare no competing financial interest.

■ ACKNOWLEDGMENTS

We thank Tres Cantos Open Lab Foundation (project TC045), GlaxoSmithKline, University of Helsinki, and the Academy of Finland (project no. 265481) for financial support. Dr. Leo Ghemti and Dr. Henri Xhaard are thanked for valuable help in computational studies during the project. The CSC–IT Center for Science Ltd. (Helsinki, Finland) and the Drug Discovery and Chemical Biology Network of the Biocenter Finland are thanked for computational resources.

■ ABBREVIATIONS

ACT, artemisinin-based combination therapy; EDC, *N*-(3-dimethylaminopropyl)-*N'*-ethylcarbodiimide hydrochloride; HOBT, 1-hydroxybenzotriazole; TCDI, 1,1'-thiocarbonyldiimidazole

■ REFERENCES

- (1) World Health Organization. *World Malaria Report 2014*; WHO Press: Geneva, Switzerland, 2014. http://www.who.int/malaria/publications/world_malaria_report_2014/report/en/ (accessed February 16, 2015).
- (2) Calderón, F.; Wilson, D. M.; Gamo, F.-J. Antimalarial Drug Discovery: Recent Progress and Future Directions. *Prog. Med. Chem.* **2013**, *52*, 97–151.
- (3) Sachs, J.; Malaney, P. The Economic and Social Burden of Malaria. *Nature* **2002**, *415*, 680–685.
- (4) Noeld, H.; Se, Y.; Schaecher, K.; Smith, B. L.; Socheat, D.; Fukuda, M. M. Evidence of Artemisinin-Resistant Malaria in Western Cambodia. *N. Engl. J. Med.* **2008**, *359*, 2619–2620.
- (5) Gamo, F.-J.; Sanz, L. M.; Vidal, J.; de Cozar, C.; Alvarez, E.; Lavandera, J.-L.; Vanderwall, D. E.; Green, D. V. S.; Kumar, V.; Hasan, S.; Brown, J. R.; Peishoff, C. E.; Cardon, L. R.; Garcia-Bustos, J. F. Thousands of Chemical Starting Points for Antimalarial Lead Identification. *Nature* **2010**, *465*, 305–310.
- (6) (a) Plouffe, D.; Brinker, A.; McNamara, C.; Henson, K.; Kato, N.; Kuhnen, K.; Nagle, A.; Adrián, F.; Matzen, J. T.; Anderson, P.; Nam, T.; Gray, N. S.; Chatterjee, A.; Janes, J.; Yan, S. F.; Trager, R.; Caldwell, J. S.; Schultz, P. G.; Zhou, Y.; Winzeler, E. A. In Silico Activity Profiling Reveals the Mechanism of Action of Antimalarials Discovered in a High-Throughput Screen. *Proc. Natl. Acad. Sci. U.S.A.* **2008**, *105*, 9059–9064. (b) Gagaring, K.; Borboa, R.; Francek, C.; Chen, X.; Buenviaje, J.; Plouffe, D.; Winzeler, E.; Brinker, A.; Diagona, T.; Taylor, J.; Glynn, R.; Chatterjee, A.; Kuhnen, K. *Novartis-GNF Malaria Box*. Genomics Institute of the Novartis Research Foundation: San Diego, CA and Novartis Institute for Tropical Disease: Singapore, 2010.
- (7) Guiguemde, W. A.; Shelat, A. A.; Bouck, D.; Duffy, S.; Crowther, G. J.; Davis, P. H.; Smithson, D. C.; Connelly, M.; Clark, J.; Zhu, F.; Jiménez-Díaz, M. B.; Martínez, M. S.; Wilson, E. B.; Tripathi, A. K.; Gut, J.; Sharlow, E. R.; Bathurst, I.; Mazouni, F. E.; Fowble, J. W.; Forquer, I.; McGinley, P. L.; Castro, S.; Angulo-Barturen, I.; Ferrer, S.; Rosenthal, P. J.; DeRisi, J. L.; Sullivan, D. J.; Lazo, J. S.; Roos, D. S.; Riscoe, M. K.; Phillips, M. A.; Rathod, P. K.; Van Voorhis, W. C.; Avery, V. M.; Guy, R. K. Chemical Genetics of *Plasmodium falciparum*. *Nature* **2010**, *465*, 311–315.
- (8) ChEMBL - Neglected Tropical Disease Database. <https://www.ebi.ac.uk/chemblntd>.
- (9) Calderón, F.; Barros, D.; Bueno, J. M.; Coterón, J. M.; Fernández, E.; Gamo, F. J.; Lavandera, J. L.; León, M. L.; Macdonald, S. J. F.; Mallo, A.; Manzano, P.; Porras, E.; Fiandor, J. M.; Castro, J. An Invitation to Open Innovation in Malaria Drug Discovery: 47 Quality Starting Points from the TCAMS. *ACS Med. Chem. Lett.* **2011**, *2*, 741–746.
- (10) Calderón, F.; Vidal-Mas, J.; Burrows, J.; de la Rosa, J. C.; Jiménez-Díaz, M. B.; Mulet, T.; Prats, S.; Solana, J.; Witty, M.; Gamo, F. J.; Fernández, E. A Divergent SAR Study Allows Optimization of a Potent 5-HT_{2c} Inhibitor to a Promising Antimalarial Scaffold. *ACS Med. Chem. Lett.* **2012**, *3*, 373–377.
- (11) Rueda, L.; Castellote, I.; Castro-Pichel, J.; Chaparro, M. J.; de la Rosa, J. C.; Garcia-Perez, A.; Gordo, M.; Jiménez-Díaz, M. B.; Kessler, A.; Macdonald, S. J. F.; Martínez, M. S.; Sanz, L. M.; Gamo, F. J.; Fernandez, E. Cyclopropyl Carboxamides: A New Oral Antimalarial Series Derived from the Tres Cantos Anti-Malarial Set (TCAMS). *ACS Med. Chem. Lett.* **2011**, *2*, 840–844.
- (12) Bansal, Y.; Silakari, O. The Therapeutic Journey of Benzimidazoles: A Review. *Bioorg. Med. Chem.* **2012**, *20*, 6208–6236.
- (13) Alp, M.; Göker, H.; Brun, R.; Yildiz, S. Synthesis and Antiparasitic and Antifungal Evaluation of 2'-Arylstubstituted-1*H*,1'*H*-[2,5']bisbenzimidazolyl-5-Carboxamidines. *Eur. J. Med. Chem.* **2009**, *44*, 2002–2008.
- (14) Roman, G.; Crandall, I. E.; Szarek, W. A. Synthesis and Antiplasmodium Activity of Benzimidazole Analogues Structurally Related to Astemizole. *ChemMedChem* **2013**, *8*, 1795–1804.
- (15) Navarrete-Vázquez, G.; de Monserrat Rojano-Vilchis, M.; Yépez-Mulia, L.; Meléndez, V.; Gerena, L.; Hernández-Campos, A.

Castillo, R.; Hernández-Luis, F. Synthesis and Antiprotozoal Activity of Some 2-(trifluoromethyl)-1H-Benzimidazole Bioisosteres. *Eur. J. Med. Chem.* **2006**, *41*, 135–141.

(16) Mohapatra, S. C.; Tiwari, H. K.; Singla, M.; Rathi, B.; Sharma, A.; Mahiya, K.; Kumar, M.; Sinha, S.; Chauhan, S. S. Antimalarial Evaluation of copper(II) Nanohybrid Solids: Inhibition of Plasmeprin II, a Hemoglobin-Degrading Malarial Aspartic Protease from *Plasmodium falciparum*. *J. Biol. Inorg. Chem.* **2010**, *15*, 373–385.

(17) Toro, P.; Klahn, A. H.; Pradines, B.; Lahoz, F.; Pascual, A.; Biot, C.; Arancibia, R. Organometallic Benzimidazoles: Synthesis, Characterization and Antimalarial Activity. *Inorg. Chem. Commun.* **2013**, *35*, 126–129.

(18) Hameed, P. S.; Chinnapattu, M.; Shanbag, G.; Manjrekar, P.; Koushik, K.; Raichurkar, A.; Patil, V.; Jatheendranath, S.; Rudrapatna, S. S.; Barde, S. P.; Rautela, N.; Awasthy, D.; Morayya, S.; Narayan, C.; Kavanagh, S.; Saralaya, R.; Bharath, S.; Viswanath, P.; Mukherjee, K.; Bhandodkar, B.; Srivastava, A.; Panduga, V.; Reddy, J.; Prabhakar, K. R.; Sinha, A.; Jiménez-Díaz, M. B.; Martínez, M. S.; Angulo-Barturen, I.; Ferrer, S.; Sanz, L. M.; Gamo, F. J.; Duffy, S.; Avery, V. M.; Magistrado, P. A.; Lukens, A. K.; Wirth, D. F.; Waterson, D.; Balasubramanian, V.; Iyer, P. S.; Narayanan, S.; Hosagrahara, V.; Sambandamurthy, V. K.; Ramachandran, S. Aminoazabenzimidazoles, a Novel Class of Orally Active Antimalarial Agents. *J. Med. Chem.* **2014**, *57*, 5702–5713.

(19) Ramachandran, S.; Hameed, P. S.; Srivastava, A.; Shanbhag, G.; Morayya, S.; Rautela, N.; Awasthy, D.; Kavanagh, S.; Bharath, S.; Reddy, J.; Panduga, V.; Prabhakar, K. R.; Saralaya, R.; Nanduri, R.; Raichurkar, A.; Menasinakai, S.; Achar, V.; Jiménez-Díaz, M. B.; Martínez, M. S.; Angulo-Barturen, I.; Ferrer, S.; Sanz, L. M.; Gamo, F. J.; Duffy, S.; Avery, V. M.; Waterson, D.; Lee, M. C. S.; Coburn-Flynn, O.; Fidock, D. A.; Iyer, P. S.; Narayanan, S.; Hosagrahara, V.; Sambandamurthy, V. K. *N*-Aryl-2-Aminobenzimidazoles: Novel, Efficacious, Antimalarial Lead Compounds. *J. Med. Chem.* **2014**, *57*, 6642–6652.

(20) Roman, G.; Crandall, I. E.; Szarek, W. A. Synthesis and Anti-Plasmodium Activity of Benzimidazole Analogues Structurally Related to Astemizole. *ChemMedChem* **2013**, *8*, 1795–1804.

(21) Keurulainen, L.; Salin, O.; Siiskonen, A.; Kern, J. M.; Alvesalo, J.; Kiuru, P.; Maass, M.; Yli-Kauhaluoma, J.; Vuorela, P. Design and Synthesis of 2-Arylbzimidazoles and Evaluation of Their Inhibitory Effect against *Chlamydia pneumoniae*. *J. Med. Chem.* **2010**, *53*, 7664–7674.

(22) Jiménez-Díaz, M. B.; Mulet, T.; Viera, S.; Gómez, V.; Garuti, H.; Ibáñez, J.; Alvarez-Doval, A.; Shultz, L. D.; Martínez, A.; Gargallo-Viola, D.; Angulo-Barturen, I. Improved Murine Model of Malaria Using *Plasmodium falciparum* Competent Strains and Non-Myelodepleted NOD-Scid IL2R γ null Mice Engrafted with Human Erythrocytes. *Antimicrob. Agents Chemother.* **2009**, *53*, 4533–4536.

(23) Lelièvre, J.; Almela, M. J.; Lozano, S.; Miguel, C.; Franco, V.; Leroy, D.; Herreros, E. Activity of Clinically Relevant Antimalarial Drugs on *Plasmodium falciparum* Mature Gametocytes in an ATP Bioluminescence “Transmission Blocking” Assay. *PloS One* **2012**, *7*, e35019.

(24) Desjardins, R. E.; Canfield, C. J.; Haynes, J. D.; Chulay, J. D. Quantitative Assessment of Antimalarial Activity *in vitro* by a Semiautomated Microdilution Technique. *Antimicrob. Agents Chemother.* **1979**, *16*, 710–718.

(25) Webster, R.; Leishman, D.; Walker, D. Towards a Drug Concentration Effect Relationship for QT Prolongation and Torsades de Pointes. *Curr. Opin. Drug Discovery Dev.* **2002**, *5*, 116–126.

(26) Bruin, M. L. D.; Pettersson, M.; Meyboom, R. H. B.; Hoes, A. W.; Leufkens, H. G. M. Anti-hERG Activity and the Risk of Drug-Induced Arrhythmias and Sudden Death. *Eur. Heart J.* **2005**, *26*, 590–597.

(27) Redfern, W. S.; Carlsson, L.; Davis, A. S.; Lynch, W. G.; MacKenzie, I.; Palethorpe, S.; Siegl, P. K. S.; Strang, I.; Sullivan, A. T.; Wallis, R.; Camm, A. J.; Hammond, T. G. Relationships between Preclinical Cardiac Electrophysiology, Clinical QT Interval Prolongation and Torsade de Pointes for a Broad Range of Drugs: Evidence for

a Provisional Safety Margin in Drug Development. *Cardiovasc. Res.* **2003**, *58*, 32–45.

(28) Crouch, S. P. M.; Kozłowski, R.; Slater, K. J.; Fletcher, J. The Use of ATP Bioluminescence as a Measure of Cell Proliferation and Cytotoxicity. *J. Immunol. Methods* **1993**, *160*, 81–88.

(29) Jiménez-Díaz, M. B.; Mulet, T.; Gómez, V.; Viera, S.; Alvarez, A.; Garuti, H.; Vázquez, Y.; Fernández, A.; Ibáñez, J.; Jiménez, M.; Gargallo-Viola, D.; Angulo-Barturen, I. Quantitative Measurement of *Plasmodium*-Infected Erythrocytes in Murine Models of Malaria by Flow Cytometry Using Bidimensional Assessment of SYTO-16 Fluorescence. *Cytometry, Part A* **2009**, *75A*, 225–235.